

# HIGH-ORDER FINITE DIFFERENCE SCHEME FOR MAXWELL'S EQUATIONS WITH INTERFACE JUMP CONDITIONS FOR COMPLEX INTERFACES

YANN-MEING LAW\*, ALEXANDRE NOLL MARQUES†, AND JEAN-CHRISTOPHE NAVE\*

**Abstract.** We propose a high-order finite-difference time-domain (FDTD) scheme based on the correction function method (CFM) to treat interfaces with complex geometry. We present a system of PDEs coming from Maxwell's equations and for which the solution corresponds to a function (the correction function) that can be used to correct the FDTD scheme in the vicinity of interfaces. We perform a perturbation analysis on the CFM's system of PDEs. A functional that is a square measure of the error satisfying the CFM's system of PDEs is minimized in a divergence-free discrete functional space. This allows us to compute an approximation of the correction function where it is needed. The approximation of the correction function is then used to correct either a second-order or fourth-order FDTD scheme. We use a staggered grid in space to enforce the discrete divergence constraints and the fourth-order Runge-Kutta time-stepping method. The discrete divergence constraint, the stability and the error of the resulting scheme are studied. Numerical experiments are performed for problems with different geometries of the interface, including one with cusps. A second-order convergence is obtained for a second-order FDTD scheme with the CFM. High-order convergence is obtained with a fourth-order FDTD scheme with the CFM. The discontinuities within the solutions are accurately captured without spurious oscillations even around cusps.

**1. Introduction.** In computational electromagnetics, the treatment of interface conditions between materials is challenging. These interface conditions arise when dielectric materials are considered, or when surface charges and currents are present at the interface. One of the main challenges is to obtain high-order accuracy schemes for arbitrarily complex interfaces, such as geometries with singularities, without increasing the complexity of the numerical scheme [8].

To handle interface conditions, various numerical strategies use the Immersed Interface Method (IIM) [11] or the Matched Interface and Boundary (MIB) method [20] for dielectric interface [6], perfectly electric conducting (PEC) boundaries [19] and Drude materials [16]. However, high-order schemes are difficult to achieve using these approaches for complex interfaces. An alternative approach is to use the correction function method (CFM) [13], which was inspired by the Ghost Fluid Method (GFM) [7]. This method was originally developed to handle Poisson's equation with interface jump conditions for arbitrarily complex interfaces. In contrast to the GFM for which high accuracy is very hard to obtain, the CFM achieves high-order accuracy by means of a minimization problem that determines the corrections to apply at each node around the interface. The CFM's minimization problem is derived as follows. A partial differential equations (PDE) for which the solution corresponds to a function (the correction function) that can be used to correct the finite difference (FD) scheme in the vicinity of interfaces is first derived based on the original PDE. A functional that is a square measure of the error satisfying the CFM's PDE is minimized on patches around the interface in an appropriate functional space. The CFM was applied on Poisson's equation with piecewise constant coefficients [14] and on the wave equation with constant coefficients [2].

In addition to the difficulties associated to the treatment of the interface, one needs to satisfy (at the discrete level) or to accurately approximate the divergence-

---

\*Department of Mathematics and Statistics, McGill University, Montréal, QC H3A 0B9, Canada. (yann-meing.law-kamcio@mcgill.ca, jean-christophe.nave@mcgill.ca)

†Department of Aeronautics and Astronautics, Massachusetts Institute of Technology, Cambridge, MA 02139-4307. (noll@mit.edu)

free constraints coming from Maxwell's equations to obtain accurate results. Many numerical methods were proposed to enforce these constraints, such as Yee's scheme [18] in finite-difference time-domain methods, local divergence-free shape functions in finite element methods [5, 4, 10] and penalization approaches [3, 15].

In this paper, we propose a high-order finite-difference time-domain scheme based on the correction function method for Maxwell's equations to treat interface conditions with complex geometries. We use a staggered finite difference (FD) scheme in space, similar to what is done for Yee's scheme, and the fourth-order Runge-Kutta method as a time-stepping method. The staggered grid in space guarantees that the nodes far from the interface satisfy the divergence constraints at the discrete level. The CFM requires a functional to be minimized in a chosen functional space. In our case, the functional coming from the correction function's PDE is minimized within a divergence-free functional space, which again enforces the divergence constraints. Two-dimensional numerical examples based on the transversal magnetic ( $\text{TM}_z$ ) mode are investigated to verify the proposed numerical strategy. The main goal of this paper is to demonstrate the feasibility to develop high-order accuracy schemes using the CFM for interfaces with arbitrarily complex geometry without increasing the complexity of the numerical scheme in the context of computational electromagnetics (CEM). Various geometries of interface are considered, such as sharp interfaces with cusps. Here we only consider problems with coefficients that vary continuously across the interface. Discontinuous coefficients introduce additional complexity in the context of the CFM, and we will address such problems in future work.

The paper is structured as follows. In [section 2](#), we define the problem, namely Maxwell's equations with interface jump conditions. The correction function method is introduced in [section 3](#). We derive the correction function's PDE coming from Maxwell's equations and perform a perturbation analysis. The minimization procedure of the discrete problem is described. The combination of the staggered finite difference scheme with the fourth-order Runge-Kutta method and the CFM is presented in [section 4](#). The error and the discrete divergence constraint are discussed, and the stability of the numerical strategy is demonstrated for an arbitrary explicit Runge-Kutta method for linear PDEs. Several two-dimensional numerical examples with complex interfaces are investigated in [section 5](#).

**2. Definition of the Problem.** Consider a domain  $\Omega$  subdivided into two subdomains  $\Omega^+$  and  $\Omega^-$  for which the interface  $\Gamma$  between the subdomains is stationary, that is it does not vary in time, and allows the solution to be discontinuous. In our case, both the tangential and normal components of the magnetic field  $\mathbf{H}$  and the electric field  $\mathbf{E}$  across the interface could be discontinuous. The jumps in the magnetic field and the electric field are denoted as

$$\begin{aligned} \llbracket \mathbf{H} \rrbracket &= \mathbf{H}^+ - \mathbf{H}^-, \\ \llbracket \mathbf{E} \rrbracket &= \mathbf{E}^+ - \mathbf{E}^-, \end{aligned}$$

where  $\mathbf{H}^+$  and  $\mathbf{E}^+$  are the solutions in  $\Omega^+$ , and  $\mathbf{H}^-$  and  $\mathbf{E}^-$  are the solutions in  $\Omega^-$ . We also consider the boundary  $\partial\Omega$  and a time interval  $I = [0, T]$ . The geometry of a typical domain is illustrated in [Figure 1](#). Assuming linear media in such a domain

and Ohm's law, Maxwell's equations are then given by

$$\begin{aligned}
 (1a) \quad & \partial_t(\mu \mathbf{H}) + \nabla \times \mathbf{E} = \mathbf{f}_1(\mathbf{x}, t) \quad \text{in } \Omega \times I, \\
 (1b) \quad & \partial_t(\epsilon \mathbf{E}) - \nabla \times \mathbf{H} = -\sigma \mathbf{E} + \mathbf{f}_2(\mathbf{x}, t) \quad \text{in } \Omega \times I, \\
 (1c) \quad & \nabla \cdot (\epsilon \mathbf{E}) = \rho \quad \text{in } \Omega \times I, \\
 (1d) \quad & \nabla \cdot (\mu \mathbf{H}) = 0 \quad \text{in } \Omega \times I, \\
 (1e) \quad & \hat{\mathbf{n}} \times \llbracket \mathbf{E} \rrbracket = 0 \quad \text{on } \Gamma \times I, \\
 (1f) \quad & \hat{\mathbf{n}} \times \llbracket \mathbf{H} \rrbracket = \mathbf{J}_s \quad \text{on } \Gamma \times I, \\
 (1g) \quad & \hat{\mathbf{n}} \cdot \llbracket \epsilon \mathbf{E} \rrbracket = \rho_s \quad \text{on } \Gamma \times I, \\
 (1h) \quad & \hat{\mathbf{n}} \cdot \llbracket \mu \mathbf{H} \rrbracket = 0 \quad \text{on } \Gamma \times I, \\
 (1i) \quad & \mathbf{n} \times \mathbf{H} = \mathbf{e}(\mathbf{x}, t) \quad \text{on } \partial\Omega \times I, \\
 (1j) \quad & \mathbf{n} \times \mathbf{E} = \mathbf{g}(\mathbf{x}, t) \quad \text{on } \partial\Omega \times I, \\
 (1k) \quad & \mathbf{H} = \mathbf{H}(\mathbf{x}, 0) \quad \text{in } \Omega, \\
 (1l) \quad & \mathbf{E} = \mathbf{E}(\mathbf{x}, 0) \quad \text{in } \Omega,
 \end{aligned}$$

where  $\mu$  is the magnetic permeability,  $\epsilon$  is the electric permittivity,  $\sigma$  is the conductivity,  $\rho$  is the electric charge density,  $\mathbf{J}_s$  is the surface current density,  $\rho_s$  is the surface charge density,  $\mathbf{n}$  is the unit outward normal to  $\partial\Omega$ ,  $\hat{\mathbf{n}}$  is the unit normal to the interface  $\Gamma$  pointing toward  $\Omega^+$ , and  $\mathbf{f}_1(\mathbf{x}, t)$  and  $\mathbf{f}_2(\mathbf{x}, t)$  are source terms. Equation (1a) to (1c) are known respectively as Faraday's law, Ampère-Maxwell's law and Gauss' law. The divergence-free constraint on the magnetic induction field is given by equation (1d). The interface conditions on  $\Gamma$  are given by equations (1e) to (1h), and the boundary conditions and the initial conditions are given by equations (1i) to (1l). In this paper, we consider more general interface conditions, given by

$$\begin{aligned}
 \hat{\mathbf{n}} \times \llbracket \mathbf{E} \rrbracket &= \mathbf{a}(\mathbf{x}, t) \quad \text{on } \Gamma \times I, \\
 \hat{\mathbf{n}} \times \llbracket \mathbf{H} \rrbracket &= \mathbf{b}(\mathbf{x}, t) \quad \text{on } \Gamma \times I, \\
 \hat{\mathbf{n}} \cdot \llbracket \epsilon \mathbf{E} \rrbracket &= c(\mathbf{x}, t) \quad \text{on } \Gamma \times I, \\
 \hat{\mathbf{n}} \cdot \llbracket \mu \mathbf{H} \rrbracket &= d(\mathbf{x}, t) \quad \text{on } \Gamma \times I,
 \end{aligned}$$

which is useful to verify the proposed numerical strategy. We also assume that the physical parameters are constant in the domain  $\Omega$  and use periodic boundary conditions. Even if the divergence constraints (1c) and (1d) seem to be redundant, it is

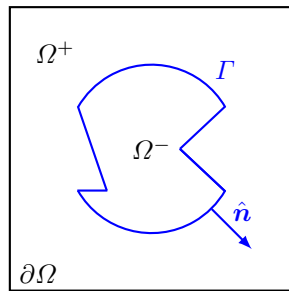


FIG. 1. Geometry of a domain  $\Omega$  with an interface  $\Gamma$ . Note that the normal  $\hat{\mathbf{n}}$  may not be well defined at the corners.

important to consider them in order to guaranty the uniqueness of the solutions [9]. As mentioned in the introduction, it also helps to obtain accurate numerical solutions.

**3. Correction Function Method.** In this section, we first present the idea behind the correction function method and the benefits of using it. We then define the governing partial differential equations for the correction functions coming from problem (1) and perform a perturbation analysis. A quadratic functional that is a square measure of the error is derived. This functional is then minimized in a discrete functional space. Particular attention is paid to the choice of the discrete functional space in order to guarantee the divergence-free constraint.

**3.1. Introduction to the CFM.** Noticing first that the solution to problem (1) is discontinuous, one cannot use *a priori* a numerical method, such as a standard finite difference method, that requires at least the solution to be in  $\mathcal{C}^1(\Omega)$ . In the following, we show how to circumvent this issue by using a correction function that extends the solutions in the different subdomains and, hence, allow us to use FD scheme.

For simplicity and without loss of generality, we show the principle behind the CFM through an 1-D example problem. Let us assume a domain  $\Omega = [x_\ell, x_r]$  divided in  $N_x$  cells. The nodes are defined as  $x_{i+1/2} = x_\ell + i \Delta x$  for  $i = 0, \dots, N_x$ , where  $\Delta x = \frac{x_r - x_\ell}{N_x}$ . For a given  $i$ , we now consider an interface  $\Gamma$  between  $x_{i-1/2} \in \Omega^+$  and  $x_{i+1/2} \in \Omega^-$ . Let us suppose we want to compute a second-order approximation of the first derivative of  $H(x)$  at the cell center  $x_i \in \Omega^+$ . We clearly have

$$\partial_x H^+(x_i) \approx \partial_x H_i^+ \neq \frac{H_{i+1/2}^- - H_{i-1/2}^+}{\Delta x}$$

because of the discontinuity at the interface  $\Gamma$ . However, assuming for the moment that we can extend the solution  $H^+$  in the domain  $\Omega^-$  in such a way that

$$\begin{aligned} \partial_x H_i^+ &= \frac{H_{i+1/2}^+ - H_{i-1/2}^+}{\Delta x} \\ &= \frac{(H_{i+1/2}^- + D_{i+1/2}) - H_{i-1/2}^+}{\Delta x} \\ &= \frac{H_{i+1/2}^- - H_{i-1/2}^+}{\Delta x} + \frac{D_{i+1/2}}{\Delta x}, \end{aligned}$$

where  $D_{i+1/2} = H_{i+1/2}^+ - H_{i+1/2}^-$  is a correction function evaluated at  $x_{i+1/2}$ . We therefore are able to compute an accurate approximation of  $\partial_x H_i^+$ . In a PDE context, the term  $\frac{D_{i+1/2}}{\Delta x}$  acts as a source term. The CFM has been applied to develop high-order FD schemes for the Poisson and wave equations with jump conditions [13, 2]. In this work, we extend the CFM to Maxwell's equations. In the next subsection, we build the governing PDE coming from Maxwell's equations (1) for which the solutions are defined as the correction function, namely  $D$  in the above 1-D example.

**3.2. Maxwell's equations CFM.** To find the PDE associated to Maxwell's equations CFM, we consider a small region  $\Omega_\Gamma$  of the domain that encloses the interface  $\Gamma$ . We assume that  $\mathbf{H}^+$ ,  $\mathbf{H}^-$ ,  $\mathbf{E}^+$ ,  $\mathbf{E}^-$  and the associated source terms can be smoothly extended in  $\Omega_\Gamma \times I$  in such a way that Maxwell's equations still be satisfied,

that is

$$\begin{aligned}
(2) \quad & \mu \partial_t \mathbf{H}^+ + \nabla \times \mathbf{E}^+ = \mathbf{f}_1^+(\mathbf{x}, t) \quad \text{in } \Omega_\Gamma \times I, \\
& \epsilon \partial_t \mathbf{E}^+ - \nabla \times \mathbf{H}^+ = -\sigma \mathbf{E}^+ + \mathbf{f}_2^+(\mathbf{x}, t) \quad \text{in } \Omega_\Gamma \times I, \\
& \quad \nabla \cdot \mathbf{E}^+ = \frac{\rho}{\epsilon} \quad \text{in } \Omega_\Gamma \times I, \\
& \quad \nabla \cdot \mathbf{H}^+ = 0 \quad \text{in } \Omega_\Gamma \times I, \\
& \mu \partial_t \mathbf{H}^- + \nabla \times \mathbf{E}^- = \mathbf{f}_1^-(\mathbf{x}, t) \quad \text{in } \Omega_\Gamma \times I, \\
& \epsilon \partial_t \mathbf{E}^- - \nabla \times \mathbf{H}^- = -\sigma \mathbf{E}^- + \mathbf{f}_2^-(\mathbf{x}, t) \quad \text{in } \Omega_\Gamma \times I, \\
& \quad \nabla \cdot \mathbf{E}^- = \frac{\rho}{\epsilon} \quad \text{in } \Omega_\Gamma \times I, \\
& \quad \nabla \cdot \mathbf{H}^- = 0 \quad \text{in } \Omega_\Gamma \times I, \\
& \quad \hat{\mathbf{n}} \times \llbracket \mathbf{E} \rrbracket = \mathbf{a}(\mathbf{x}, t) \quad \text{on } \Gamma \times I, \\
& \quad \hat{\mathbf{n}} \times \llbracket \mathbf{H} \rrbracket = \mathbf{b}(\mathbf{x}, t) \quad \text{on } \Gamma \times I, \\
& \quad \hat{\mathbf{n}} \cdot \llbracket \epsilon \mathbf{E} \rrbracket = c(\mathbf{x}, t) \quad \text{on } \Gamma \times I, \\
& \quad \hat{\mathbf{n}} \cdot \llbracket \mu \mathbf{H} \rrbracket = d(\mathbf{x}, t) \quad \text{on } \Gamma \times I.
\end{aligned}$$

Subtracting from the equations for  $\mathbf{H}^+$  and  $\mathbf{E}^+$  the equations for  $\mathbf{H}^-$  and  $\mathbf{E}^-$  of system (2), we obtain the following system of equations

$$\begin{aligned}
(3a) \quad & \mu \partial_t \mathbf{D}_H + \nabla \times \mathbf{D}_E = \mathbf{f}_{D_1}(\mathbf{x}, t) \quad \text{in } \Omega_\Gamma \times I, \\
(3b) \quad & \epsilon \partial_t \mathbf{D}_E - \nabla \times \mathbf{D}_H = -\sigma \mathbf{D}_E + \mathbf{f}_{D_2}(\mathbf{x}, t) \quad \text{in } \Omega_\Gamma \times I, \\
(3c) \quad & \nabla \cdot \mathbf{D}_E = 0 \quad \text{in } \Omega_\Gamma \times I, \\
(3d) \quad & \nabla \cdot \mathbf{D}_H = 0 \quad \text{in } \Omega_\Gamma \times I, \\
(3e) \quad & \hat{\mathbf{n}} \times \mathbf{D}_E = \mathbf{a}(\mathbf{x}, t) \quad \text{on } \Gamma \times I, \\
(3f) \quad & \hat{\mathbf{n}} \times \mathbf{D}_H = \mathbf{b}(\mathbf{x}, t) \quad \text{on } \Gamma \times I, \\
(3g) \quad & \hat{\mathbf{n}} \cdot \mathbf{D}_E = c(\mathbf{x}, t) \quad \text{on } \Gamma \times I, \\
(3h) \quad & \hat{\mathbf{n}} \cdot \mathbf{D}_H = d(\mathbf{x}, t) \quad \text{on } \Gamma \times I,
\end{aligned}$$

which determine the correction function  $\mathbf{D}_H = \llbracket \mathbf{H} \rrbracket$  and  $\mathbf{D}_E = \llbracket \mathbf{E} \rrbracket$ . The source terms are given by  $\mathbf{f}_{D_1} = \mathbf{f}_1^+ - \mathbf{f}_1^-$  and  $\mathbf{f}_{D_2} = \mathbf{f}_2^+ - \mathbf{f}_2^-$ . The interface conditions (1e) to (1h) become boundary conditions (3e) to (3h) for system (3).

**3.3. Perturbation analysis of Maxwell's equations CFM.** In this subsection, a perturbation analysis of the correction function's PDE coming from Maxwell's equations is investigated using a standard Fourier analysis for initial value problem following the same procedure described in [13, 2]. The correction function's PDE is not always well-posed. An example of such a situation is Poisson problems for which the CFM leads to an ill-posed Cauchy problem [13].

In the following, we only focus on the first two equations of (3) because the divergence constraint is naturally satisfied by an appropriate choice of the functional space in which we minimize the quadratic functional (see subsection 3.4). We suppose, without loss of generality, that the interface is flat and is parallel to the  $xy$ -plane and  $\mathbf{x} = 0 \in \Gamma$ . Let us also define the distance  $d$  from the interface, which is along the positive part of the  $z$ -axis in the subdomain  $\Omega^+$ . We therefore have an orthogonal coordinate system  $(\mathbf{y}, d)$ , where  $\mathbf{y} = [x, y]^T$  spans the interface and  $d = z$ . Assume that the physical parameters are such that  $\mu > 0$ ,  $\epsilon > 0$  and  $\sigma > 0$ . Consider a

periodic domain  $\Omega = [-\pi, \pi]^3$ , we search solutions for small perturbations of  $\mathbf{D}_H$  and  $\mathbf{D}_E$  on the interface, namely  $\tilde{\mathbf{D}}_H$  and  $\hat{\mathbf{D}}_H$ , of the form

$$(4) \quad \tilde{\mathbf{U}}(\mathbf{x}, t) = \sum_{k_x, k_y, k_z \in \mathbb{Z}} \hat{\mathbf{U}}_{k_x, k_y, k_z}(t) e^{i \mathbf{k} \cdot \mathbf{x}},$$

where  $\tilde{\mathbf{U}} = [\tilde{\mathbf{D}}_H^T \ \hat{\mathbf{D}}_E^T]^T$  and  $\mathbf{k} = [k_x, k_y, k_z]^T$ . Substitute (4) into the first two equations of (3) with  $\mathbf{f}_{D_1} = \mathbf{f}_{D_2} = 0$  leads to a system of ordinary differential equations (ODE) for each coefficient, given by :

$$\partial_t \hat{\mathbf{U}}_{k_x, k_y, k_z} = A \hat{\mathbf{U}}_{k_x, k_y, k_z}$$

with

$$A = \begin{bmatrix} 0 & 0 & 0 & 0 & i k_z / \mu & -i k_y / \mu \\ 0 & 0 & 0 & -i k_z / \mu & 0 & i k_x / \mu \\ 0 & 0 & 0 & i k_y / \mu & -i k_x / \mu & 0 \\ 0 & -i k_z / \epsilon & i k_y / \epsilon & -\sigma / \epsilon & 0 & 0 \\ i k_z / \epsilon & 0 & -i k_x / \epsilon & 0 & -\sigma / \epsilon & 0 \\ -i k_y / \epsilon & i k_x / \epsilon & 0 & 0 & 0 & -\sigma / \epsilon \end{bmatrix}.$$

Depending on the values of  $\mathbf{k} \cdot \mathbf{k}$ , we have three cases:

- 1) If  $\mathbf{k} \cdot \mathbf{k} = 0$ , we have  $\mathbf{k} = 0$  and the matrix  $A$  has two distinct eigenvalues  $\lambda_1 = 0$  and  $\lambda_2 = -\frac{\sigma}{\epsilon}$ . It is easy to show that  $\dim(\ker(A - \lambda_i I)) = 3$  for  $i = 1, 2$ , and that  $B = [\mathbf{s}_1 \dots \mathbf{s}_6] = I$ , where  $\mathbf{s}_j$  for  $j = 1, \dots, 6$  denotes an eigenvector. Hence, we have six linearly independent eigenvectors.
- 2) If  $\mathbf{k} \cdot \mathbf{k} = \frac{\mu \sigma^2}{4 \epsilon}$ , the matrix  $A$  has three distinct eigenvalues  $\lambda_1 = 0$ ,  $\lambda_2 = -\frac{\sigma}{\epsilon}$  and  $\lambda_3 = -\frac{\sigma}{2 \epsilon}$ . We have  $\dim(\ker(A - \lambda_1 I)) = \dim(\ker(A - \lambda_2 I)) = 1$ . However, the multiplicity of  $\lambda_3$  is four, but  $\dim(\ker(A - \lambda_3 I)) = 2$ . We therefore need to find two other solutions of the form  $\mathbf{c} = \mathbf{s} t + \mathbf{b}$  associated to the eigenvectors given by  $\lambda_3$ . Using a standard method to solve an ODE with multiple eigenvalues, we find

$$\det(B) = \frac{\epsilon^2 \sigma^2 \mu}{k_z^2 (4 \epsilon k_y^2 + 4 \epsilon k_z^2 - \mu \sigma^2)} \neq 0,$$

where  $B = [\mathbf{s}_1 \dots \mathbf{s}_4 \ \mathbf{c}_1 \ \mathbf{c}_2]$ .

- 3) Otherwise, the matrix  $A$  has four distinct eigenvalues given by  $\lambda_1 = 0$ ,  $\lambda_2 = -\frac{\sigma}{\epsilon}$  and

$$\lambda_{3,4} = \frac{-\sigma \mu \pm \sqrt{\mu(4 \epsilon \mathbf{k} \cdot \mathbf{k} - \mu \sigma^2)} i}{2 \epsilon \mu}.$$

We have  $\dim(\ker(A - \lambda_i)) = 1$  for  $i = 1, 2$ , and  $\dim(\ker(A - \lambda_i)) = 2$  for  $i = 3, 4$ . We therefore have

$$\det(B) = \frac{\mathbf{k} \cdot \mathbf{k} (4 \epsilon \mathbf{k} \cdot \mathbf{k} - \mu \sigma^2)}{\mu k_x^2 k_z^2} \neq 0.$$

For all cases, it is possible to obtain a general solution of the form

$$\hat{\mathbf{U}}_{k_x, k_y, k_z}(t) = \sum_i \mathbf{a}_i e^{\lambda_i t},$$

where the vectors  $\mathbf{a}_i$  are computed using given initial conditions of the small perturbations and the eigenvectors. Since  $\sigma > 0$  and  $\epsilon > 0$ , there is no exponential growth of the form  $e^{at}$  with  $a > 0$ . Hence, the problem coming from the first two equations of (3) does not allow perturbations to growth. A perturbation of  $\mathbf{D}_H$  and  $\mathbf{D}_E$  on the interface  $\Gamma$  is therefore unchanged, dispersed and/or diffused.

REMARK 1. For highly resistive medium, it is common to consider  $\sigma = 0$ . In this case, if  $\mathbf{k} \cdot \mathbf{k} \neq 0$ , the matrix  $A$  has three distinct eigenvalues  $\lambda_1 = 0$  and

$$\lambda_{2,3} = \pm \sqrt{\frac{\mathbf{k} \cdot \mathbf{k}}{\epsilon \mu}} i.$$

Following the same procedure than the one for  $\sigma > 0$ , we find that the problem coming from the first two equations of (3) does not allow perturbations to growth.

**3.4. Discretization of Maxwell's equations CFM.** In this subsection, we define a local patch  $\Omega_\Gamma^h \subset \Omega_\Gamma$ , where the correction functions, namely  $\mathbf{D}_H$  and  $\mathbf{D}_E$ , need to be computed at a node  $(\mathbf{x}, t) \in \Omega_\Gamma^h$ . The approximations of the correction functions within a patch are obtained by minimizing a quadratic functional.

The definition of a patch is a slight modification of the ‘‘Node Centered’’ technique [13]. As in the ‘‘Node Centered’’ approach, we define a patch for each node that needs to be corrected. However, we restrict the patch to be squared and aligned with the computational grid. We now summarize the procedure to compute  $\Omega_\Gamma^h$ . For a given node  $\mathbf{x}_c$  that needs to be corrected, we find an approximation of the point  $\mathbf{p}$  on the interface  $\Gamma$  that is the closest to  $\mathbf{x}_c$ . We construct a square centered at  $\mathbf{p}$  of length  $\ell_h = \beta \max\{\Delta x, \Delta y, \Delta z\}$  where  $\beta$  is a positive constant. The parameter  $\beta$  depends on the FD scheme and it is chosen to ensure that  $\mathbf{x}_c \in \Omega_\Gamma^h$ . For exemple,  $\beta = 1$  and  $\beta = 3$  for respectively the second-order and the fourth-order staggered FD scheme presented in section 4. This construction of the patch guarantees the uniqueness of a correction function at each node and is important for the conservation of the discrete divergence constraint for some nodes close to  $\Gamma$  (see Theorem 4.3).

Let us now present the functional to be minimized in order to obtain approximations of the correction functions. We begin by introducing some notations. The inner product in  $L^2(\Omega_\Gamma^h \times [t_n, t_{n+1}])$  is defined by

$$\langle \mathbf{v}, \mathbf{w} \rangle = \int_{t_n}^{t_{n+1}} \int_{\Omega_\Gamma^h} \mathbf{v} \cdot \mathbf{w} \, dV \, dt.$$

For legibility, we also use the notation

$$\langle \mathbf{v}, \mathbf{w} \rangle_\Gamma = \int_{t_n}^{t_{n+1}} \int_{\Gamma \cap \Omega_\Gamma^h} \mathbf{v} \cdot \mathbf{w} \, dS \, dt.$$

To compute an approximation of the correction functions  $\mathbf{D}_H$  and  $\mathbf{D}_E$ , we consider

the following quadratic functional to minimize

$$\begin{aligned}
J(\mathbf{D}_H, \mathbf{D}_E) &= \frac{\ell_c}{2} \langle \mu \partial_t \mathbf{D}_H + \nabla \times \mathbf{D}_E - \mathbf{f}_{D_1}, \mu \partial_t \mathbf{D}_H + \nabla \times \mathbf{D}_E - \mathbf{f}_{D_1} \rangle \\
&+ \frac{\ell_c}{2} \langle \epsilon \partial_t \mathbf{D}_E - \nabla \times \mathbf{D}_H + \sigma \mathbf{D}_E - \mathbf{f}_{D_2}, \epsilon \partial_t \mathbf{D}_E - \nabla \times \mathbf{D}_H + \sigma \mathbf{D}_E - \mathbf{f}_{D_2} \rangle \\
&+ \frac{1}{2} \langle \hat{\mathbf{n}} \times \mathbf{D}_H - \mathbf{b}, \hat{\mathbf{n}} \times \mathbf{D}_H - \mathbf{b} \rangle_\Gamma + \frac{1}{2} \langle \hat{\mathbf{n}} \cdot \mathbf{D}_H - d, \hat{\mathbf{n}} \cdot \mathbf{D}_H - d \rangle_\Gamma \\
&+ \frac{1}{2} \langle \hat{\mathbf{n}} \times \mathbf{D}_E - \mathbf{a}, \hat{\mathbf{n}} \times \mathbf{D}_E - \mathbf{a} \rangle_\Gamma + \frac{1}{2} \langle \hat{\mathbf{n}} \cdot \mathbf{D}_E - c, \hat{\mathbf{n}} \cdot \mathbf{D}_E - c \rangle_\Gamma,
\end{aligned}$$

where  $\ell_c > 0$  is a scale factor and  $[t_n, t_{n+1}]$  is a time interval. The scale factor  $\ell_c$  is chosen to ensure that all the terms in the functional  $J$  behave in a similar way when the computational grid is refined (see [Remark 3](#)). As one can observe, we do not consider explicitly the divergence-free constraint [\(3c\)](#) and [\(3d\)](#). These constraints are naturally satisfied by an appropriate choice of the polynomial spaces in which we minimize the functional  $J$ . The problem statement is then

$$(5) \quad \text{Find } (\mathbf{D}_H, \mathbf{D}_E) \in V \times W \text{ such that } (\mathbf{D}_H, \mathbf{D}_E) \in \underset{\mathbf{v} \in V, \mathbf{w} \in W}{\arg \min} J(\mathbf{v}, \mathbf{w}),$$

where  $V$  and  $W$  are two divergence-free polynomial spaces that is

$$V = \{ \mathbf{v} \in [P^k(\Omega_\Gamma^h \times [t_n, t_{n+1}])]^3 : \nabla \cdot \mathbf{v} = 0 \},$$

where  $P^k$  denotes the space of polynomials of degree  $k$ , and  $V = W$ . The space-time basis functions of  $V$  are obtained using the tensor product between the basis functions of  $P^k([t_n, t_{n+1}])$  and the basis functions of

$$\tilde{V} = \{ \mathbf{v} \in [P^k(\Omega_\Gamma^h)]^3 : \nabla \cdot \mathbf{v} = 0 \}.$$

Computing the Gateaux derivative and using the necessary condition to obtain a minimum, we have the following problem :

Find  $(\mathbf{D}_H, \mathbf{D}_E) \in V \times W$  such that

$$\left\{ \begin{array}{l}
\ell_c \langle \mu^2 \partial_t \mathbf{D}_H + \mu \nabla \times \mathbf{D}_E - \mu \mathbf{f}_{D_1}, \partial_t \mathbf{v} \rangle - \ell_c \langle \epsilon \partial_t \mathbf{D}_E + \nabla \times \mathbf{D}_H - \sigma \mathbf{D}_E + \mathbf{f}_{D_2}, \nabla \times \mathbf{v} \rangle \\
+ \langle \hat{\mathbf{n}} \times \mathbf{D}_H - \mathbf{b}, \hat{\mathbf{n}} \times \mathbf{v} \rangle_\Gamma + \langle \hat{\mathbf{n}} \cdot \mathbf{D}_H - d, \hat{\mathbf{n}} \cdot \mathbf{v} \rangle_\Gamma = 0, \quad \forall \mathbf{v} \in V, \\
\ell_c \langle \mu \partial_t \mathbf{D}_H + \nabla \times \mathbf{D}_E - \mathbf{f}_{D_1}, \nabla \times \mathbf{w} \rangle + \ell_c \langle \epsilon^2 \partial_t \mathbf{D}_E - \epsilon \nabla \times \mathbf{D}_H + \sigma \mathbf{D}_E - \mathbf{f}_{D_2}, \partial_t \mathbf{w} \rangle \\
+ \langle \epsilon \partial_t \mathbf{D}_E - \sigma \nabla \times \mathbf{D}_H + \sigma^2 \mathbf{D}_E - \sigma \mathbf{f}_{D_2}, \mathbf{w} \rangle \\
+ \langle \hat{\mathbf{n}} \times \mathbf{D}_E - \mathbf{a}, \hat{\mathbf{n}} \times \mathbf{w} \rangle_\Gamma + \langle \hat{\mathbf{n}} \cdot \mathbf{D}_E - c, \hat{\mathbf{n}} \cdot \mathbf{w} \rangle_\Gamma = 0, \quad \forall \mathbf{w} \in W.
\end{array} \right.$$

**REMARK 2.** For simplicity, consider the 1-D version of system [\(3\)](#) with  $\sigma = 0$  and without source term, it can be shown that the information is propagated at a speed of  $\frac{1}{\sqrt{\epsilon\mu}}$  as it is well-known for homogeneous Maxwell's equations with  $\sigma = 0$  and  $\rho = 0$ . This gives us an insight on how to choose the time-step size. For the general case, we choose a time-step size for the CFM that is  $\Delta t \approx \sqrt{\epsilon\mu} \ell_h$  to allow the informations coming from the interface  $\Gamma$  to propagate in the whole local patch  $\Omega^h$ .

**REMARK 3.** Consider a square patch of length  $\ell_h$  and  $\Delta t = \mathcal{O}(\ell_h)$ . Using discrete

polynomial spaces  $P^k$ , the correction functions are  $(k+1)$ -order accurate and we have

$$\begin{aligned}\mu \partial_t \mathbf{D}_H + \nabla \times \mathbf{D}_E - \mathbf{f}_{D_1} &= \mathcal{O}(\ell_h^k), \\ \epsilon \partial_t \mathbf{D}_E - \nabla \times \mathbf{D}_H + \sigma \mathbf{D}_E - \mathbf{f}_{D_2} &= \mathcal{O}(\ell_h^k), \\ \hat{\mathbf{n}} \times \mathbf{D}_E - \mathbf{a} &= \mathcal{O}(\ell_h^{k+1}), \\ \hat{\mathbf{n}} \times \mathbf{D}_H - \mathbf{b} &= \mathcal{O}(\ell_h^{k+1}), \\ \hat{\mathbf{n}} \cdot \mathbf{D}_E - c &= \mathcal{O}(\ell_h^{k+1}), \\ \hat{\mathbf{n}} \cdot \mathbf{D}_H - d &= \mathcal{O}(\ell_h^{k+1}).\end{aligned}$$

Substituting these terms in the functional  $J$ , we find that the terms  $\langle \cdot, \cdot \rangle$  and  $\langle \cdot, \cdot \rangle_\Gamma$  behave respectively as  $\mathcal{O}(\ell_c \ell_h^{2k+4})$  and  $\mathcal{O}(\ell_h^{2k+5})$ . Hence, we need  $\ell_c = \ell_h$  to have all the terms converging in a similar way when the computational grid is refined.

REMARK 4. The computational cost of minimization problems for the CFM is not small. However, only the nodes around the interface need a correction. Assuming an uniform mesh of  $N^d$  nodes, where  $d$  is the dimension and  $N$  is the number of nodes used in each dimension, the computational cost scales as  $N^{d-1}$  [13]. For large problems, this cost then becomes less significant. Moreover, it has been show that a parallel implementation of the CFM can help to overcome this issue [1] and make the CFM suitable for more complex problems.

REMARK 5. In this work, 2-D numerical examples are investigated. We use a similar procedure proposed by [5] to generate the basis functions of  $\tilde{V}$ . Besides being at divergence-free, the dimension of  $\tilde{V}$ , given by  $\frac{(k+1)(k+4)}{2}$ , is smaller than the dimension of  $[P^k(\Omega_\Gamma^h)]^2$  given by  $(k+1)(k+2)$ . This reduces the computational cost of the CFM.

**4. 2-D Staggered Discretization.** Considering the transverse magnetic (TM<sub>z</sub>) mode, the magnetic field is therefore given by  $\mathbf{H}(\mathbf{x}, t) = (H_x(x, y, t), H_y(x, y, t), 0)$  and the electric field by  $\mathbf{E}(\mathbf{x}, t) = (0, 0, E_z(x, y, t))$ . For a domain  $\Omega \subset \mathbb{R}^2$  and constant physical parameters, problem (1) is then simplified to

$$\begin{aligned}\mu \partial_t H_x + \partial_y E_z &= f_{1_x} \quad \text{in } \Omega \times I, \\ \mu \partial_t H_y - \partial_x E_z &= f_{1_y} \quad \text{in } \Omega \times I, \\ \epsilon \partial_t E_z - \partial_x H_y + \partial_y H_x &= -\sigma E_z + f_2 \quad \text{in } \Omega \times I, \\ \partial_x H_x + \partial_y H_y &= 0 \quad \text{in } \Omega \times I,\end{aligned}$$

with the associated interface, boundary and initial conditions.

REMARK 6. In this work, we demonstrate the feasibility of the numerical strategy in 2-D using the TM<sub>z</sub> mode. From a conceptual point of view, there is, in principle, no additional difficulties if one chooses the transverse electric (TE<sub>z</sub>) mode or a fully 3-D problem as long as  $\rho = 0$ . However, the implementation for a fully 3-D problem is more involved due to the treatment of the interface which is a surface in 3-D. It is worth noting that recent progress has been made to ease the implementation of the CFM in 3-D [12].

**4.1. Numerical Scheme.** Let us now define the staggered space discretization which is similar to what is done in space for Yee's scheme. For simplicity, we consider the rectangular domain  $\Omega \in [x_\ell, x_r] \times [y_b, y_t]$ . The nodes of the grid are defined as

$$(x_{i+1/2}, y_{j+1/2}) = (x_\ell + i \Delta x, y_b + j \Delta y)$$

for  $i = 0, 1, \dots, N_x$  and  $j = 0, 1, \dots, N_y$  with  $\Delta x := (x_r - x_\ell)/N_x$  and  $\Delta y := (y_r - y_b)/N_y$ . We also define the center of a cell  $\Omega_{i,j} = [x_{i-1/2}, x_{i+1/2}] \times [y_{j-1/2}, y_{j+1/2}]$  by

$$(x_i, y_i) = (x_\ell + (i - \frac{1}{2}) \Delta x, y_b + (j - \frac{1}{2}) \Delta y)$$

for  $i = 1, \dots, N_x$  and for  $j = 1, \dots, N_y$ . The midpoints of edges parallel to the  $x$ -axis and those parallel to the  $y$ -axis are respectively defined as

$$(x_i, y_{j+1/2}) = (x_\ell + (i - \frac{1}{2}) \Delta x, y_b + j \Delta y)$$

for  $i = 1, \dots, N_x$  and for  $j = 0, \dots, N_y$ , and

$$(x_{i+1/2}, y_j) = (x_\ell + i \Delta x, y_b + (j - \frac{1}{2}) \Delta y)$$

for  $i = 0, \dots, N_x$  and for  $j = 1, \dots, N_y$ . For time discretization, the time interval  $I = [0, T]$  is subdivided into  $N_t$  subintervals of length  $\Delta t := T/N_t$ . Unlike the space discretization, we do not staggered the variables in time. The components of the magnetic field are then approximated at the edges of the cell that is

$$H_x(x_i, y_{j+1/2}, t_n) \approx H_{x,i,j+1/2}^n$$

and

$$H_y(x_{i+1/2}, y_j, t_n) \approx H_{y,i+1/2,j}^n,$$

and the  $z$ -component of the electric field is approximated at the center of the cell

$$E_z(x_i, y_j, t_n) \approx E_{z,i,j}^n.$$

The spatial derivatives are computed using either a second-order or a fourth-order approximation. For example, a fourth-order approximation of  $\partial_x H_y(x_i, y_j, t_n)$  is given by

$$(6) \quad \frac{H_{y,i-3/2,j}^n - 27 H_{y,i-1/2,j}^n + 27 H_{y,i+1/2,j}^n - H_{y,i+3/2,j}^n}{24 \Delta x}.$$

For time discretization, we use the fourth-order Runge-Kutta (RK4) method, which is given by

$$(7) \quad \mathbf{U}^{n+1} = \mathbf{U}^n + \frac{1}{6} (\mathbf{k}_1 + 2 \mathbf{k}_2 + 2 \mathbf{k}_3 + \mathbf{k}_4),$$

with  $\mathbf{U}^n = [H_x^n, H_y^n, E_z^n]^T$ ,

$$\begin{aligned} \mathbf{k}_1 &= \Delta t \mathbf{G}(t_n, \mathbf{U}^n), \\ \mathbf{k}_2 &= \Delta t \mathbf{G}(t_n + \frac{\Delta t}{2}, \mathbf{U}^n + \frac{\mathbf{k}_1}{2}), \\ \mathbf{k}_3 &= \Delta t \mathbf{G}(t_n + \frac{\Delta t}{2}, \mathbf{U}^n + \frac{\mathbf{k}_2}{2}), \\ \mathbf{k}_4 &= \Delta t \mathbf{G}(t_n + \Delta t, \mathbf{U}^n + \mathbf{k}_3), \end{aligned}$$

and

$$(8) \quad \mathbf{G}(t_n, \mathbf{U}^n) = \begin{bmatrix} \frac{1}{\mu} (f_{1_x}^n - \partial_{y_h} E_z^n) \\ \frac{1}{\mu} (f_{1_y}^n + \partial_{x_h} E_z^n) \\ -\sigma E_z^n + f_2^n + \partial_{x_h} H_y^n - \partial_{y_h} H_x^n \end{bmatrix},$$

where the subscript  $h$  in the spatial derivatives denotes a given finite difference approximation of them in  $\Omega$ . Let us now consider a FD approximation of the spatial derivatives for which we apply correction functions, that is  $D_{H_x}$ ,  $D_{H_y}$  and  $D_{E_z}$ . It has been shown that a direct interpolation of the approximation of the correction functions at times  $t_n$ ,  $t_{n+1/2}$  and  $t_{n+1}$ , which are needed for the different stages of the RK4 method, results in a suboptimal second-order accurate approximation in time. As proposed in [2], we need to slightly modify the approximation of the correction functions to regain a full fourth-order approximation in time. Based on Taylor expansions, the modified approximation of the correction functions at each stage are

$$\begin{aligned} \text{1st stage :} & \quad \hat{D}_1^n = D^n, \\ \text{2nd stage :} & \quad \hat{D}_2^n \approx D^n + \frac{\Delta t}{2} \partial_t D^n, \\ \text{3rd stage :} & \quad \hat{D}_3^n \approx D^n + \frac{\Delta t}{2} \partial_t D^n + \frac{\Delta t^2}{4} \partial_t^2 D^n, \\ \text{4th stage :} & \quad \hat{D}_4^n \approx D^n + \Delta t \partial_t D^n + \frac{\Delta t^2}{2} \partial_t^2 D^n + \frac{\Delta t^3}{4} \partial_t^3 D^n, \end{aligned}$$

where  $D^n = [D_{H_x}^n, D_{H_y}^n, D_{E_z}^n]^T$ . The time derivatives of the correction functions can be computed directly using their polynomial approximations coming from the minimization problem (5).

**4.2. Error Analysis.** In this short subsection, we study the impact of the approximation of the correction functions on the finite difference scheme. As shown in Lemma 4.1, the error associated to the approximation of the correction function coming from the minimization problem (5) can reduce the order of convergence of the original finite difference scheme, that is without correction.

LEMMA 4.1. *For sufficiently smooth functions  $A(x)$  and  $D(x)$ , assume that the approximation of the correction function  $D$  is  $p$ -order accurate and the fourth-order centered FD scheme, namely*

$$(9) \quad \partial_x A_i = \frac{A_{i-3/2} - 27 A_{i-1/2} + 27 A_{i+1/2} - A_{i+3/2}}{24 \Delta x}.$$

*The order of convergence of the fourth-order centered FD scheme when a correction is applied is  $q = \min\{p - 1, 4\}$ .*

*Proof.* Consider that the fourth-order centered FD scheme (9) involves approximations of  $A$  that belongs to different subdomains. For simplicity and without loss of generality, suppose that  $x_i \in \Omega^+$  and only one node belongs to the domain  $\Omega^-$ , that is  $x_{i+1/2} \in \Omega^-$  and  $x_{i-3/2}, x_{i-1/2}, x_{i+3/2} \in \Omega^+$ . Hence, we have

$$(10) \quad \partial_x A_i^+ = \frac{A_{i-3/2}^+ - 27 A_{i-1/2}^+ + 27 (A_{i+1/2}^- + D_{i+1/2}) - A_{i+3/2}^+}{24 \Delta x},$$

where  $D_{i+1/2}$  is the approximation of the correction function evaluated at  $x_{i+1/2}$ . Since the approximation of the correction function is  $p$ -order accurate,

$$D(x_{i+1/2}) = D_{i+1/2} + \mathcal{O}(\Delta x^p).$$

Using appropriate Taylor's expansions about  $x_i$  of  $A_{i+1/2}^-$  and  $D(x_{i+1/2})$ , we find

$$\begin{aligned}
(11) \quad A_{i+1/2}^- + D_{i+1/2} &= A_{i+1/2}^- + D(x_{i+1/2}) + \mathcal{O}(\Delta x^p) \\
&= \sum_{j=0}^{\infty} \frac{1}{2^j j!} \left( \partial_x^{(j)} A^-(x_i) + \partial_x^{(j)} D(x_i) \right) \Delta x^j + \mathcal{O}(\Delta x^p) \\
&= \sum_{j=0}^{\infty} \frac{1}{2^j j!} \partial_x^{(j)} A^+(x_i) \Delta x^j + \mathcal{O}(\Delta x^p).
\end{aligned}$$

Using (11) and performing a standard Taylor's expansion of (10) about  $x_i$ , we find

$$\partial_x A_i^+ = \partial_x A^+(x_i) + \mathcal{O}(\Delta x^4 + \Delta x^{p-1}).$$

□

**4.3. Discrete Divergence Constraint.** In this subsection, we discuss about the conservation of the discrete divergence of the finite difference scheme combined with the CFM. We first show that the standard FD scheme preserves the divergence of the initial data at the discrete level. Secondly, we show that the discrete divergence is still conserved for the FD scheme when combined with the CFM except for some nodes close to the interface.

A common second-order discrete approximation of the divergence of a 2-D vector field is computed using

$$(12) \quad (\nabla \cdot \mathbf{A})_{i+1/2, j+1/2}^n := \frac{A_{x, i+1, j+1/2}^n - A_{x, i, j+1/2}^n}{\Delta x} + \frac{A_{y, i+1/2, j+1}^n - A_{y, i+1/2, j}^n}{\Delta y},$$

where  $\mathbf{A} = [A_x, A_y, 0]^T$  [17]. We also introduce a centered fourth-order discrete approximation of the divergence, given by

$$\begin{aligned}
(13) \quad (\tilde{\nabla} \cdot \mathbf{A})_{i+1/2, j+1/2}^n &:= \frac{A_{x, i-1, j+1/2}^n - 27 A_{x, i, j+1/2}^n + 27 A_{x, i+1, j+1/2}^n - A_{x, i+2, j+1/2}^n}{24 \Delta x} \\
&\quad + \frac{A_{y, i+1/2, j-1}^n - 27 A_{y, i+1/2, j}^n + 27 A_{y, i+1/2, j+1}^n - A_{y, i+1/2, j+2}^n}{24 \Delta y},
\end{aligned}$$

which is better suited for our fourth-order scheme.

For the  $\text{TM}_z$  mode, we remark that the electric field  $\mathbf{E}(\mathbf{x}, t) = (0, 0, E(x, y, t))$  is divergence free. We then focus on the magnetic field. The following lemma shows that the standard staggered finite difference scheme combined with the RK4 time-stepping method preserves the discrete divergence of the initial data at all later times.

LEMMA 4.2. *Assume that the source terms satisfy*

$$(\tilde{\nabla} \cdot \mathbf{f}_1)_{i+1/2, j+1/2}^n = 0,$$

*for all  $i, j$  and all  $n \geq 0$ . The magnetic field, computed with the standard fourth-order staggered FD scheme combined with the RK4 method, is such that*

$$(\tilde{\nabla} \cdot \mathbf{H})_{i+1/2, j+1/2}^{n+1} = (\tilde{\nabla} \cdot \mathbf{H})_{i+1/2, j+1/2}^0,$$

*for all  $i, j$  and all  $n \geq 0$ .*

*Proof.* The following demonstration is similar to the proof given in [17]. For a given time  $t_n$ , let us consider the two first components of (8), that is

$$\mathbf{G}_H(t^n, E_z^n) = \frac{1}{\mu} \begin{bmatrix} f_{1_x}^n - \partial_{y_h} E_z^n \\ f_{1_y}^n + \partial_{x_h} E_z^n \end{bmatrix},$$

where  $\partial_{y_h} \cdot$  and  $\partial_{x_h} \cdot$  denote the centered fourth-order approximation derivative (6). Applying the discrete divergence operator to  $\mathbf{G}_H(t^n, E_z^n)$  leads to

$$(\tilde{\nabla} \cdot \mathbf{G}_H)_{i+1/2, j+1/2}^n = (\tilde{\nabla} \cdot \mathbf{f}_1)_{i+1/2, j+1/2}^n + (\tilde{\nabla} \cdot \mathbf{A})_{i+1/2, j+1/2}^n,$$

where

$$A_{x, i, j+1/2}^n = -\frac{E_{z, i, j-1}^n - 27 E_{z, i, j}^n + 27 E_{z, i, j+1}^n - E_{z, i, j+2}^n}{24 \Delta y},$$

$$A_{y, i+1/2, j}^n = \frac{E_{z, i-1, j}^n - 27 E_{z, i, j}^n + 27 E_{z, i+1, j}^n - E_{z, i+2, j}^n}{24 \Delta x},$$

which is a fourth-order approximation of the curl of the electric field at the cell edges. We can easily verify that

$$(\tilde{\nabla} \cdot \mathbf{A})_{i+1/2, j+1/2}^n = 0, \quad \forall i, j, n.$$

Using  $(\tilde{\nabla} \cdot \mathbf{f}_1)_{i+1/2, j+1/2}^n = 0$ , we obtain

$$(\tilde{\nabla} \cdot \mathbf{G}_H)_{i+1/2, j+1/2}^n = 0,$$

for all  $i, j$  and all  $n \geq 0$ . Applying the discrete divergence operator to (7), we find  $(\nabla \cdot \mathbf{H})_{i+1/2, j+1/2}^{n+1} = (\nabla \cdot \mathbf{H})_{i+1/2, j+1/2}^n$ . Hence, we obtain the desired result.  $\square$

Due to possible discontinuities at the interface  $\Gamma$ , we need to investigate the discrete divergence for the nodes that are closed to  $\Gamma$ . We distinguish two cases that are illustrated in Figure 2. In the first case, we consider that the discrete divergence

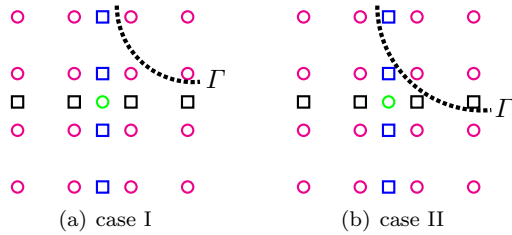


FIG. 2. Illustration of the two cases for the computation of the fourth-order divergence of the magnetic field around the interface  $\Gamma$  (dotted line). For legibility, we only show the nodes involve in Theorem 4.3 and Theorem 4.4 for the computation of the discrete divergence of  $\mathbf{H}$  at the node represented by  $\circ$ . The components  $H_x$ ,  $H_y$  and  $E_z$  are respectively represented by  $\square$ ,  $\square$  and  $\circ$ .

operator involves only components of the magnetic field that belong to the same subdomain. However, there is no restriction on the electric field. In contrast, the second case considers  $H_x$  and  $H_y$  that belong to different subdomains in the computation of the discrete divergence operator. In that situation, the discrete divergence operators (12) and (13) are not well suited and need to be redefined. In the spirit of

the CFM, we propose a corrected discrete divergence operator that uses correction functions if it is necessary. The corrected discrete divergence operator is denoted as either  $(\nabla^D \cdot \mathbf{A})_{i+1/2, j+1/2}^n$  or  $(\tilde{\nabla}^D \cdot \mathbf{A})_{i+1/2, j+1/2}^n$  for respectively a second and fourth order approximation. The following theorems analyze the discrete divergence of the approximation of  $\mathbf{H}$  in both situations.

**THEOREM 4.3.** *Under the assumption of Lemma 4.2 and assuming that the approximation of the correction function  $\hat{D}_{E_z}$  at each node is unique. If the computation of  $(\tilde{\nabla} \cdot \mathbf{H})_{i+1/2, j+1/2}^{\circ, n+1}$ , where the superscript  $\circ$  can be either  $+$  or  $-$  depending in which subdomain ( $\Omega^+$  or  $\Omega^-$ ) the node  $(x_{i+1/2}, y_{j+1/2})$  belongs, involves only approximations of the magnetic field in the same subdomain, then the approximation of  $\mathbf{H}$ , computed with the fourth-order staggered FD scheme combined with the RK4 method and the CFM, is such that*

$$(\tilde{\nabla} \cdot \mathbf{H})_{i+1/2, j+1/2}^{\circ, n+1} = (\tilde{\nabla} \cdot \mathbf{H})_{i+1/2, j+1/2}^{\circ, 0},$$

for all  $i, j$  and all  $n \geq 0$ .

*Proof.* Let us consider that the discrete divergence operator (13) involves only approximations of  $H_x$  and  $H_y$  in the same subdomain than the node  $(x_{i+1/2}, y_{j+1/2})$ . For simplicity and without loss of generality, consider that the corner where the discrete divergence operator is computed belongs to  $\Omega^+$ . Suppose that some of the approximations of the electric field in (8) belong to  $\Omega^-$ . Using the uniqueness of the correction functions and repeating the same procedure as in Lemma 4.2, but with the correction function, that is

$$E_{z, i, j}^{+, n} \mapsto E_{z, i, j}^{-, n} + \hat{D}_{E_z, i, j}^n$$

at the nodes  $(x_i, y_j, t_n)$  where it is needed, we find the desired result.  $\square$

**THEOREM 4.4.** *Assume that the correction functions, namely  $D_{H_x}$  and  $D_{H_y}$ , and the magnetic field  $\mathbf{H}$  satisfy the assumptions of Lemma 4.1, and a CFL condition of the form*

$$\Delta t = \alpha \min\{\Delta x, \Delta y\},$$

where  $\alpha$  is a positive constant. The approximation of  $\mathbf{H}$ , computed with the fourth-order staggered FD scheme combined with the RK4 method and the CFM, is such that

$$(\tilde{\nabla}^D \cdot \mathbf{H})_{i+1/2, j+1/2}^{\circ, n} = \nabla \cdot \mathbf{H}(x_{i+1/2}, y_{j+1/2}, t_n) + \mathcal{O}(\Delta x^r + \Delta y^r + \Delta t^s),$$

for all  $i, j$  and all  $n \geq 0$ , where  $r = \min\{p - 2, 3\}$ ,  $s = \min\{p - 1, 3\}$  and the superscript  $\circ$  can be either  $+$  or  $-$  depending in which subdomain ( $\Omega^+$  or  $\Omega^-$ ) the node  $(x_{i+1/2}, y_{j+1/2})$  belongs.

*Proof.* Consider that the corrected discrete divergence operator involves approximations of the components of  $\mathbf{H}$  that belong to different subdomains. For simplicity and without loss of generality, suppose that the corner, where the corrected discrete divergence operator is computed, belongs to  $\Omega^+$ . For a given time  $t_n$ , assume that we need a correction on  $H_{x, i+2, j+1/2}^{+, n}$  and  $H_{y, i+1/2, j+2}^{+, n}$  in the computation of  $(\tilde{\nabla}^D \cdot \mathbf{H})_{i+1/2, j+1/2}^{+, n}$ , that is

$$\begin{aligned} H_{x, i+2, j+1/2}^{+, n} &\approx H_{x, i+2, j+1/2}^{-, n} + D_{H_x, i+2, j+1/2}^n, \\ H_{y, i+1/2, j+2}^{+, n} &\approx H_{y, i+1/2, j+2}^{-, n} + D_{H_y, i+1/2, j+2}^n. \end{aligned}$$

Let us compute the Taylor expansion associated to  $H_{x,i+2,j+1/2}^{+,n}$ . By [Lemma 4.1](#), using a fourth-order FD scheme combined with the RK4 method and a  $p$ -order accurate approximation of the correction functions leads to

$$H_{x,i+2,j+1/2}^{+,n} \approx H_x^-(x_{i+2}, y_{j+1/2}, t_n) + \mathcal{O}(\Delta x^q + \Delta y^q + \Delta t^4) + D_{H_x}^n_{x,i+2,j+1/2},$$

where  $q = \min\{p-1, 4\}$ . Hence,

$$\begin{aligned} H_{x,i+2,j+1/2}^{+,n} &= H_x^-(x_{i+2}, y_{j+1/2}, t_n) + D_{H_x}(x_{i+2}, y_{j+1/2}, t_n) \\ (14) \quad &+ \mathcal{O}(\Delta x^q + \Delta y^q + \Delta t^4 + \Delta t^p) \\ &= H_x^+(x_{i+2}, y_{j+1/2}, t_n) + \mathcal{O}(\Delta x^q + \Delta y^q + \Delta t^k), \end{aligned}$$

where  $k = \min\{p, 4\}$ . Using a similar procedure, we also have

$$(15) \quad H_{y,i+1/2,j+2}^{+,n} = H_y^+(x_{i+1/2}, y_{j+2}, t_n) + \mathcal{O}(\Delta x^q + \Delta y^q + \Delta t^k).$$

Using a CFL condition and substituting (14) and (15) in  $(\tilde{\nabla}^D \cdot \mathbf{H})_{i+1/2,j+1/2}^{+,n}$  and using appropriate Taylor expansions, we find the desired results.  $\square$

**REMARK 7.** *Similar statements can be obtained with the second-order staggered FD scheme. However, we need to consider the second-order discrete divergence operator (12).*

**4.4. Stability.** In this subsection, we present the general explicit  $s$ -stage RK method when combined with a FD scheme and the CFM, and we discuss about its stability. For a linear PDE, [Theorem 4.5](#) shows that the proposed numerical strategy is stable if the combination of the explicit RK method and the FD scheme (without the CFM) is stable.

Let us first introduce the general  $s$ -stage explicit Runge-Kutta method, given by

$$\mathbf{U}^{n+1} = \mathbf{U}^n + \Delta t \sum_{i=1}^s b_i \mathbf{G}(\mathbf{Y}_i, t_n + c_i \Delta t),$$

where

$$\begin{aligned} \mathbf{Y}_1 &= \mathbf{U}^n, \\ \mathbf{Y}_i &= \mathbf{U}^n + \Delta t \sum_{j=1}^{i-1} a_{ij} \mathbf{G}(\mathbf{Y}_j, t_n + c_j \Delta t) \end{aligned}$$

for  $i = 2, \dots, s$ , and  $a_{ij}$ ,  $b_i$  and  $c_i$  are given coefficients.

Assume now a linear PDE and a correction function  $\hat{\mathbf{D}}$  that need to be compute at each stage. For simplicity, we do not consider source terms. We therefore obtain

$$(16) \quad \mathbf{U}^{n+1} = \mathbf{U}^n + \Delta t \sum_{i=1}^s b_i A(\mathbf{Y}_i + \hat{\mathbf{D}}_i^n),$$

where

$$(17) \quad \begin{aligned} \mathbf{Y}_1 &= \mathbf{U}^n, \\ \mathbf{Y}_i &= \mathbf{U}^n + \Delta t \sum_{j=1}^{i-1} a_{ij} A(\mathbf{Y}_j + \hat{\mathbf{D}}_j^n) \end{aligned}$$

for  $i = 2, \dots, s$ , and  $A$  is the matrix coming from a FD discretization of a linear PDE. It is now obvious that we can split (17) as

$$\mathbf{Y}_i = \mathbf{Y}_i^* + \mathbf{Y}_i^D,$$

for  $i = 1, \dots, s$ , where  $\mathbf{Y}_i^D$  contains all the correction functions and  $\mathbf{Y}_i^*$  contains all the other terms. In the case of  $\mathbf{Y}_1$ , we have  $\mathbf{Y}_1^D = 0$ . Regrouping all similar terms in equation (16) leads to

$$\begin{aligned} \mathbf{U}^{n+1} &= \mathbf{U}^n + \Delta t \sum_{i=1}^s b_i A (\mathbf{Y}_i^* + \mathbf{Y}_i^D + \hat{\mathbf{D}}_i^n) \\ (18) \quad &= \mathbf{U}^n + \Delta t \sum_{i=1}^s b_i A \mathbf{Y}_i^* + \Delta t \sum_{i=1}^s b_i A (\mathbf{Y}_i^D + \hat{\mathbf{D}}_i^n) \\ &= M \mathbf{U}^n + \sum_{i=1}^s M_i^D \hat{\mathbf{D}}_i^n. \end{aligned}$$

One can notice that  $\mathbf{U}^{n+1} = M \mathbf{U}^n$  corresponds to the explicit  $s$ -stage RK method without any corrections, which is named explicit RK-FD scheme. The following theorem ensures that the stability of the proposed strategy, namely the combination of an explicit RK-FD scheme with the CFM, is stable if the explicit RK-FD scheme is stable.

**THEOREM 4.5.** *Let us consider an explicit RK-FD scheme of the form*

$$(19) \quad \mathbf{U}^{n+1} = M \mathbf{U}^n,$$

where  $n \geq 0$ ,  $\mathbf{U}^n$  is an approximation of the solution at  $t_n$  and  $M$  is a difference matrix that approximates a linear PDE in a domain  $\Omega$ . Assume that (19) is stable, that is, for a given mesh grid size  $h$ ,

$$\|M^n\| \leq C, \quad \forall n \Delta t \leq T,$$

where  $T$  is a given time and  $C$  is a positive constant. Consider that the approximation of the correction functions at each stage  $j$  is bounded

$$\|\hat{\mathbf{D}}_j^n\| \leq C_D, \quad \forall n \Delta t \leq T$$

and for  $j = 1, \dots, s$ , where  $C_D$  is a positive constant. The combination of the explicit RK-FD scheme (19) and the CFM is then stable.

*Proof.* Consider an explicit RK-FD scheme with the CFM given by (18). For a given time  $t_{n-1}$ , we have

$$(20) \quad \mathbf{U}^n = M^n \mathbf{U}^0 + \sum_{i=0}^{n-1} \left( M^{n-1-i} \sum_{j=1}^s M_j^D \hat{\mathbf{D}}_j^i \right).$$

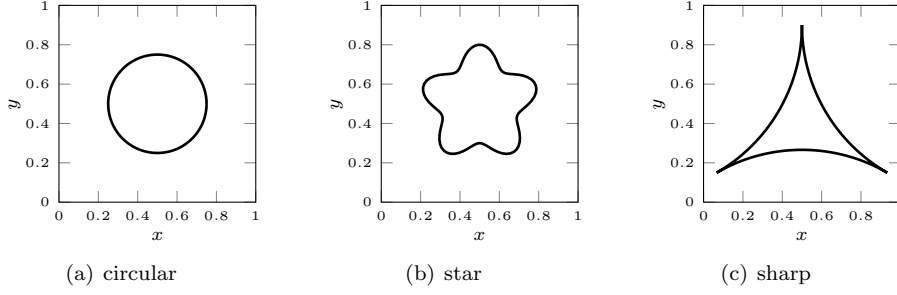


FIG. 3. *The different geometries of the interface.*

Applying the norm on (20) for which FD scheme (19) is stable, we obtain

$$\begin{aligned}
\|\mathbf{U}^n\| &\leq \|M^n\| \|\mathbf{U}^0\| + \sum_{i=0}^{n-1} \left( \|M^{n-1-i}\| \left\| \sum_{j=1}^s M_j^D \hat{D}_j^i \right\| \right) \\
&\leq \|M^n\| \|\mathbf{U}^0\| + \sum_{i=0}^{n-1} (C_D \|M^{n-i-1}\| \sum_{j=1}^s \|M_j^D\|) \\
&\leq C \left( \|\mathbf{U}^0\| + n C_D \sum_{j=1}^s \|M_j^D\| \right).
\end{aligned}$$

One can notice that the matrix  $M_j^D$  is a matrix polynomial with respect to  $A$  of degree at most  $s$ . Since the matrix  $A$  comes from a FD discretization of a PDE, we have  $\|A\| \leq C_A$  and  $\|A^s\| \leq C_A^s$ , where  $C_A$  is a positive constant. Thus,

$$\|M_j^D\| = \left\| \sum_{i=0}^s p_{ij} A^i \right\| \leq \sum_{i=0}^s |p_{ij}| C_A^i,$$

where  $p_{ij}$  are given coefficients that depend on  $a_{ij}$  and  $b_i$ . Hence, the explicit RK-FD scheme combined with the CFM is stable.  $\square$

REMARK 8. *In our case, the assumption of a bounded correction functions at each stage  $\hat{D}_j$  is appropriate because the PDE coming from Maxwell's equations does not allow perturbations to growth (see subsection 3.3).*

**5. Numerical Examples.** In the following, we perform convergence analysis of the proposed numerical schemes for problems with a manufactured solution with various interfaces. We use a fourth-order approximation of the correction functions with the RK4 method and either a second-order or a fourth-order staggered FD scheme. The domain is  $\Omega = [0, 1] \times [0, 1]$  and the time interval is  $I = [0, 0.5]$ . The physical parameters are  $\mu = \sigma = \epsilon = 1$  in all  $\Omega$ . Periodic boundary conditions are imposed on all  $\partial\Omega$  for all numerical experiments. We also choose the mesh grid size to be  $h \in \left\{ \frac{1}{20}, \frac{1}{28}, \frac{1}{52}, \frac{1}{72}, \frac{1}{96}, \frac{1}{132}, \frac{1}{180}, \frac{1}{244}, \frac{1}{336} \right\}$  and  $\Delta x = \Delta y = h$ . The time-step size is chosen to satisfy a CFL condition and to reach exactly the final time, that is  $\Delta t = \frac{h}{2}$ . Figure 3 illustrates the different geometries of the interface that are studied in this work. We have  $\phi(x, y) \geq 0$  in  $\Omega^+$ ,  $\phi(x, y) < 0$  in  $\Omega^-$  and  $\phi(x, y) = 0$  on  $\Gamma$ , where  $\phi(x, y)$  is the level-set function.

**5.1. Circular interface.** The level set function

$$\phi(x, y) = (x - x_0)^2 + (y - y_0)^2 - r_0^2,$$

where  $x_0 = y_0 = 0.5$  and  $r_0 = 0.25$ , is used to describe the interface. The manufactured solutions are :

$$\begin{aligned} H_x^+ &= \sin(2\pi x) \sin(2\pi y) \sin(2\pi t), \\ H_y^+ &= \cos(2\pi x) \cos(2\pi y) \sin(2\pi t), \\ E_z^+ &= \sin(2\pi x) \cos(2\pi y) \cos(2\pi t) \end{aligned}$$

in  $\Omega^+$ , and

$$\begin{aligned} H_x^- &= -2 \sin(2\pi x) \sin(2\pi y) \sin(2\pi t) + 5, \\ H_y^- &= -2 \cos(2\pi x) \cos(2\pi y) \sin(2\pi t) + 3, \\ E_z^- &= -2 \sin(2\pi x) \cos(2\pi y) \cos(2\pi t) + 2 \end{aligned}$$

in  $\Omega^-$ . The associated source terms are  $\mathbf{f}_1^+ = \mathbf{f}_1^- = 0$  and

$$\begin{aligned} f_2^+ &= (2\pi \sin(2\pi t) + \cos(2\pi t)) \sin(2\pi x) \cos(2\pi y), \\ f_2^- &= -(4\pi \sin(2\pi t) + 2 \cos(2\pi t)) \sin(2\pi x) \cos(2\pi y) + 2. \end{aligned}$$

Figure 4(a) and Figure 4(b) illustrate the convergence plots for respectively a second-order and a fourth-order staggered FD scheme using the  $L_\infty$ -norm and the  $L_1$ -norm. For the second-order scheme, a second-order convergence is obtained for the components  $H_x$ ,  $H_y$  and  $E_z$  in both norms as expected by Lemma 4.1. The divergence constraint converges to second and third order using respectively the  $L_\infty$ -norm and the  $L_1$ -norm, which is better than expected and still in agreement with the theory. For the fourth-order scheme, the magnetic field and the electric field converge to third-order in  $L_\infty$ -norm, while a fourth-order convergence is obtained in  $L_1$ -norm. A second and third order convergence is observed for the divergence of  $\mathbf{H}$  in  $L_\infty$ -norm and the  $L_1$ -norm. These results support our previous analysis presented in section 4. Figure 5 shows the components  $H_x$ ,  $H_y$  and  $E_z$  at different time steps using the smallest mesh grid size, namely  $h = \frac{1}{336}$ , using the fourth-order staggered FD scheme with the CFM. The discontinuities are accurately captured without spurious oscillations.

**5.2. Star interface.** The level set function is given by

$$\phi(x, y) = (x - x_0)^2 + (y - y_0)^2 - r^2(\theta),$$

where

$$r(\theta) = r_0 + \epsilon \sin(5\theta(x, y)),$$

$x_0 = y_0 = 0.5$ ,  $r_0 = 0.25$ ,  $\epsilon = 0.05$  and  $\theta(x, y)$  is the angle between the vector  $[x - x_0, y - y_0]^T$  and the  $x$ -axis. Figure 3(b) illustrates the geometry of the interface.

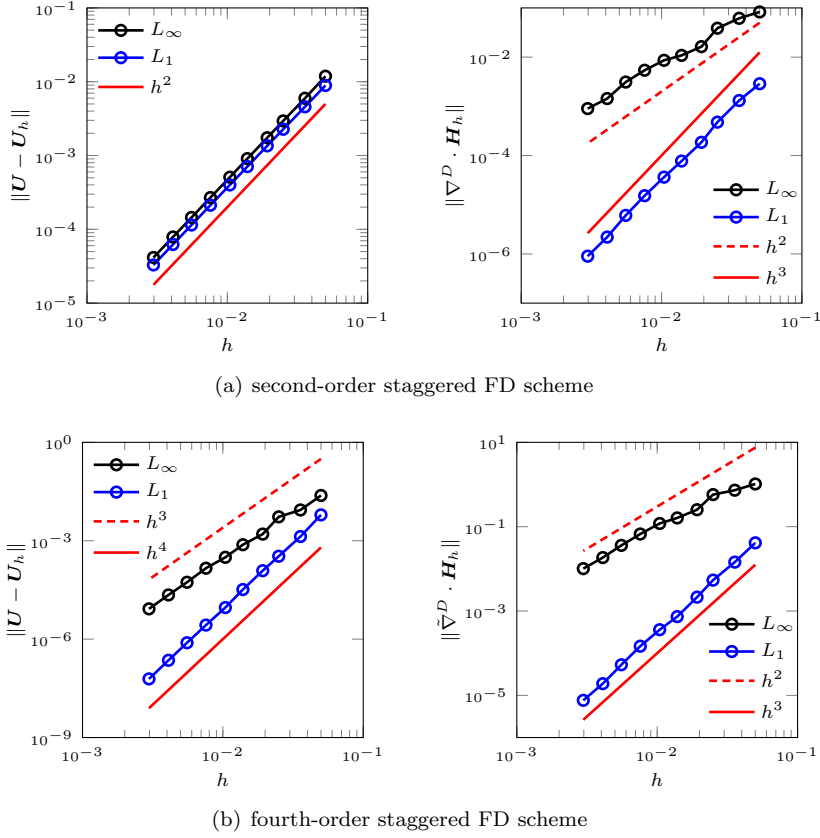


FIG. 4. Convergence plots for the problem with a manufactured solution and the circular interface using a fourth-order approximation of the correction functions, and either a second-order or fourth-order staggered FD scheme. It is recalled that  $\mathbf{U} = [H_x, H_y, E_z]^T$ .

The manufactured solutions are :

$$\begin{aligned}
 H_x^+ &= \sin(4\pi x) \sin(4\pi y) \cos(2\pi t), \\
 H_y^+ &= \cos(4\pi x) \cos(4\pi y) \cos(2\pi t), \\
 E_z^+ &= 0, \\
 H_x^- &= (-x e^{-xy} + 2) \sin(2\pi t), \\
 H_y^- &= (y e^{-xy} + 3) \sin(2\pi t), \\
 E_z^- &= \sin(2\pi xy) \cos(2\pi t).
 \end{aligned}$$

The associated source terms are

$$\begin{aligned}
f_{1_x}^+ &= -2\pi \sin(4\pi x) \sin(4\pi y) \sin(2\pi t), \\
f_{1_x}^- &= (2\pi(-x e^{-xy} + 2) + 2\pi x \cos(2\pi xy)) \cos(2\pi t), \\
f_{1_y}^+ &= -2\pi \cos(4\pi x) \cos(4\pi y) \sin(2\pi t), \\
f_{1_y}^- &= 2\pi(y e^{-xy} - y \cos(2\pi xy) + 3) \cos(2\pi t), \\
f_2^+ &= 8\pi \sin(4\pi x) \cos(4\pi y) \cos(2\pi t), \\
f_2^- &= (-2\pi \sin(2\pi xy) + y^2 e^{-xy} + x^2 e^{-xy}) \sin(2\pi t) + \sin(2\pi xy) \cos(2\pi t).
\end{aligned}$$

Figure 6 illustrates the convergence plots for a fourth-order approximation of the correction functions, and either a second-order or a fourth-order staggered FD scheme. A second-order convergence for the solutions is obtained with the second-order FD scheme in both norms, while a second and third order convergence for the divergence constraint is observed with respectively the  $L_\infty$ -norm and the  $L_1$ -norm. For the fourth-order FD scheme, the solutions converge to third and fourth order in respectively  $L_\infty$ -norm and  $L_1$ -norm. We also observe a second-order convergence for the divergence constraint using the  $L_\infty$ -norm and a third-order convergence using the  $L_1$ -norm. Figure 7 shows the evolution of the components  $H_x$ ,  $H_y$  and  $E_z$ . Here again, the discontinuities are accurately captured for a more complex interface.

**5.3. Sharp interface.** We use the same manufactured solution than the circular interface problem (see subsection 5.1). However, we choose an interface with cusps as illustrated in Figure 3(c). This interface is built using three circles of radius  $r = \frac{\sqrt{3}}{2}$  centered at  $(0.5 + r, 0.9)$ ,  $(0.5 - r, 0.9)$  and  $(0.5, -0.6)$ . Figure 8 illustrates the convergence plots for both schemes using the  $L_\infty$ -norm and the  $L_1$ -norm. For the second-order scheme, we obtain a second-order convergence for  $H_x$ ,  $H_y$  and  $E_z$ , even if the geometry has cusps. The divergence constraint converges to second and third order in respectively  $L_\infty$ -norm and  $L_1$ -norm, which better than expected. Using  $L_1$ -norm,  $H_x$ ,  $H_y$  and  $E_z$  converge to fourth-order, while a third-order convergence is obtained for the divergence of the magnetic field. The convergence orders for the sharp interface are similar to those obtained with the circular interface. Thus, the geometry of the interface does not seem to influence the convergence of the proposed numerical strategy. Figure 9 shows the magnetic field and the electric field at two different time steps using  $h = \frac{1}{336}$ , and a fourth-order staggered FD scheme with the CFM. The discontinuities are accurately captured even around the cusps.

**6. Conclusions.** This work uses the correction function method to develop high-order finite-difference time-domain schemes to handle Maxwell's equations with complex interface conditions. The system of PDEs for which the solution corresponds to the correction function is derived from Maxwell's equations with interface conditions. We have shown that this system of PDEs does not allow a perturbation on the solution to growth. A functional that is a square measure of the error associated to the correction function's system of PDEs is minimized to allow us to compute an approximation of the correction function where it is needed. A discrete divergence-free polynomial space in which the functional is minimized is chosen to satisfy the divergence constraints. The approximation of the correction function is then used to correct either a second-order or fourth-order staggered FD scheme. We use a staggered grid in space to enforce the discrete divergence constraints and the fourth-order Runge-Kutta time-stepping method. The discrete divergence constraint, the stability

and the error of the resulting scheme have been studied. We have shown that the approximation of the magnetic field remains at divergence-free for a discrete measure of the divergence, except for some nodes around the interface. We have also shown that the CFM preserves the stability of the considered FD scheme for a linear PDE and an arbitrary explicit Runge-Kutta method. Numerical experiments have been performed in 2-D using different geometries of the interface. We use a fourth-order accurate approximation of the correction functions with the fourth-order Runge-Kutta method, and either a second or fourth order staggered FD scheme. All the convergence studies are in agreement with the theory. A second-order convergence is obtained with the second-order staggered FD scheme with the CFM for all the numerical examples. We also have observed a better convergence order of the divergence-free constraint than expected. For the fourth-order staggered FD scheme with the CFM, a second and third order convergence is observed respectively for the divergence-free constraint and the solutions in  $L_\infty$ -norm, while a third and fourth order convergence is obtained in  $L_1$ -norm. The geometry of the interface does not influence the convergence rate, even the one with cusps. In all our numerical experiments, the discontinuities within the solutions are accurately captured without spurious oscillations. The proposed numerical strategy is a promising candidate to handle Maxwell's equations with interface conditions without increasing its complexity for arbitrary geometries of the interface and keeping high-order accuracy. Future work will include discontinuous coefficients to handle more realistic materials, such as dielectrics, and an extension of the proposed numerical strategy in 3-D.

**Acknowledgments.** The authors are grateful to Professor Charles Audet for interesting and helpful conversations.

#### REFERENCES

- [1] D. S. ABRAHAM AND D. D. GIANNACOPOULOS, A parallel implementation of the correction function method for Poisson's equation with immersed surface charges, IEEE Trans. Magn., 53 (2017).
- [2] D. S. ABRAHAM, A. N. MARQUES, AND J.-C. NAVE, A correction function method for the wave equation with interface jump conditions, J. Comput. Phys., 353 (2018), pp. 281–299.
- [3] F. ASSOUS, P. DEGOND, E. HEINTZE, P.A.RAVIART, AND J. SEGRE, On a finite-element method for solving the three-dimensional Maxwell equations, J. Comput. Phys., 109 (1993), pp. 222–237.
- [4] S. C. BRENNER, F. LI, AND L.-Y. SUNG, A locally divergence-free interior penalty method for two-dimensional curl-curl problems, SIAM J. Num. Anal., 46 (2008), pp. 1190–1211.
- [5] B. COCKBURN, F. LI, AND C.-W. SHU, Locally divergence-free discontinuous Galerkin methods for the Maxwell equations, J. Comput. Phys., 194 (2004), pp. 588–610.
- [6] S. DENG, On the immersed interface method for solving time-domain Maxwell's equations in materials with curved dielectric interfaces, Comput. Phys. Commun., 179 (2008), pp. 791–800.
- [7] R. P. FEDKIW, T. ASLAM, B. MERRIMAN, AND S. OSHER, A non-oscillatory eulerian approach to interfaces in multimaterial flows (the ghost fluid method), J. Comput. Phys., 152 (1999), pp. 457–492.
- [8] J. S. HESTHAVEN, High-order accurate methods in time-domain computational electromagnetics: a review, Adv. Imag. Electron Phys., 127 (2003), pp. 59–123.
- [9] B. JIANG, J. WU, AND L. POVINELLI, The origin of spurious solutions in computational electromagnetics, J. Comput. Phys., 125 (1996), pp. 104 – 123.
- [10] J.-M. JIN, The Finite Element Method in Electromagnetics, John Wiley & Sons, 2014.
- [11] R. J. LEVEQUE AND Z. LI, The immersed interface method for elliptic equations with discontinuous coefficients and singular sources, SIAM J. Num. Anal., 31 (1994), pp. 1019–1044.
- [12] A. N. MARQUES, J.-C. NAVE, AND R. R. ROSALES, Imposing jump conditions on nonconforming interfaces via least squares minimization, J. Comput. Phys., submitted for publication,

- arXiv:1710.11016.
- [13] A. N. MARQUES, J.-C. NAVE, AND R. R. ROSALES, A correction function method for Poisson problems with interface jump conditions, J. Comput. Phys., 230 (2011), pp. 7567–7597.
  - [14] A. N. MARQUES, J.-C. NAVE, AND R. R. ROSALES, High order solution of Poisson problems with piecewise constant coefficients and interface jumps, J. Comput. Phys., 335 (2017), pp. 497–515.
  - [15] C.-D. MUNZ, P. OMNES, R. SCHNEIDER, E. SONNENDRÜCKER, AND U. VOSS, Divergence correction techniques for Maxwell solvers based on a hyperbolic model, J. Comput. Phys., 161 (2000), pp. 484–511.
  - [16] D. D. NGUYEN AND S. ZHAO, A new high order dispersive FDTD method for Drude material with complex interfaces, J. Comput. Appl. Math., 289 (2015), pp. 1–14.
  - [17] G. TÓTH, The  $\nabla \cdot \mathbf{B} = 0$  constraint in shock-capturing magnetohydrodynamics codes, J. Comput. Phys., 161 (2000), pp. 605–652.
  - [18] K. S. YEE, Numerical solution of initial boundary value problems involving Maxwell’s equations in isotropic media, IEEE Trans. Antennas Propag., 14 (1966), pp. 302–307.
  - [19] S. ZHAO, A fourth order finite difference method for waveguides with curved perfectly conducting boundaries, Comput. Methods Appl. Mech. Engrg., 199 (2010), pp. 2655–2662.
  - [20] S. ZHAO AND G. W. WEI, High-order FDTD methods via derivative matching for Maxwell’s equations with material interfaces, J. Comput. Phys., 200 (2004), pp. 60–103.

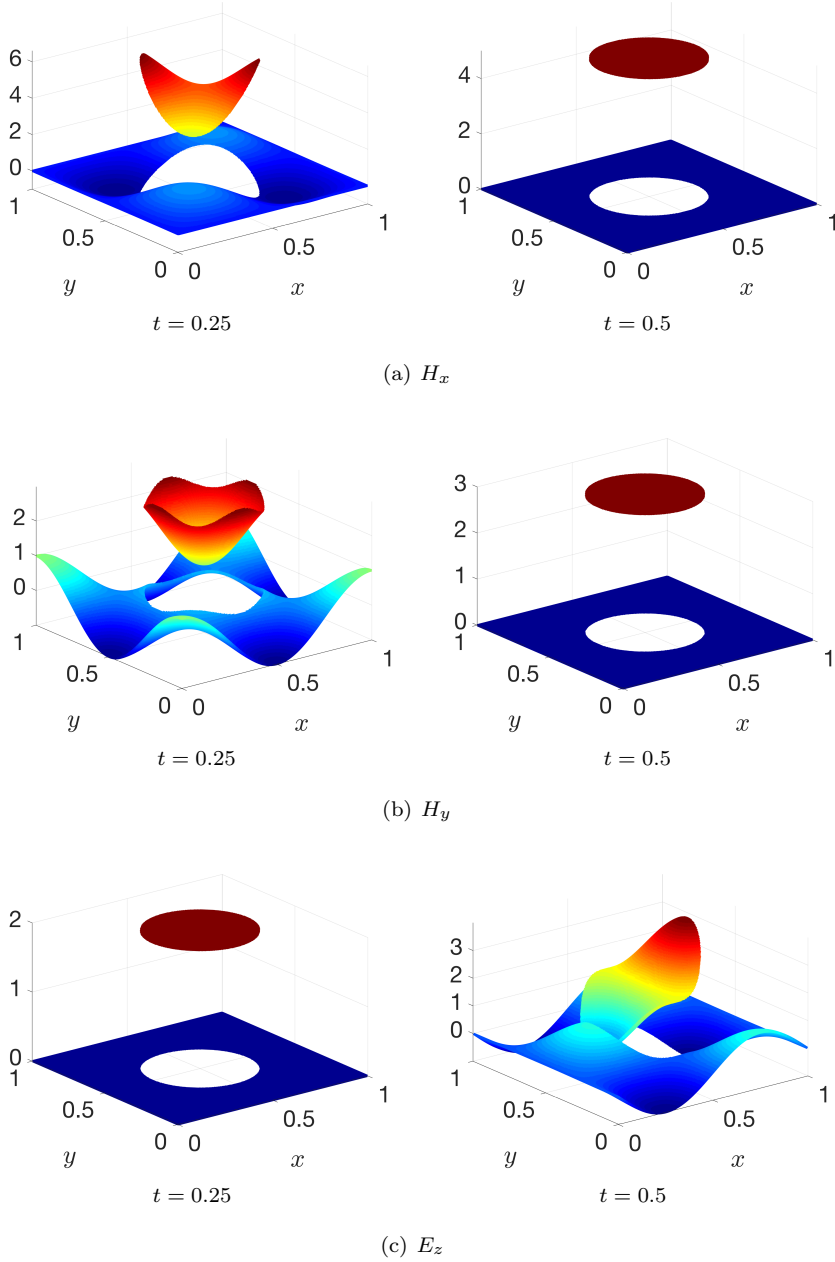
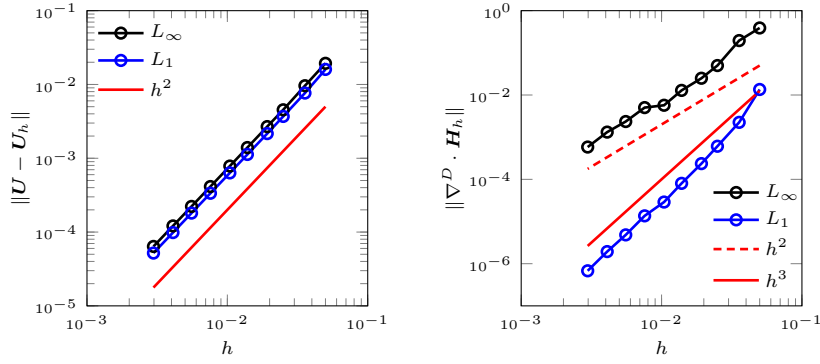
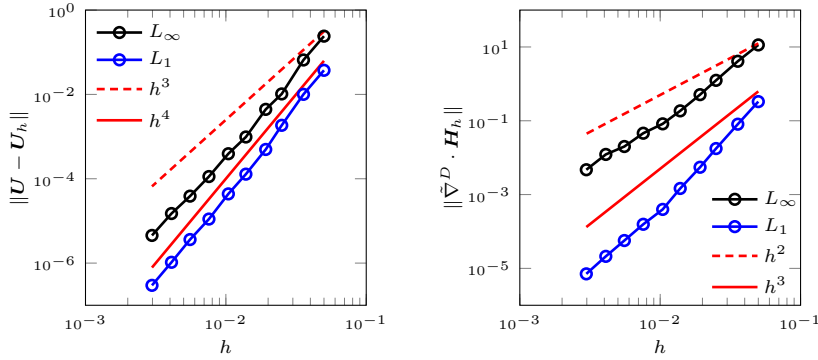


FIG. 5. The components  $H_x$ ,  $H_y$  and  $E_z$  at two time steps with  $h = \frac{1}{336}$  and  $\Delta t = \frac{h}{2}$  using a fourth-order FDTD scheme with the CFM for the problem with a manufactured solution and the circle interface.

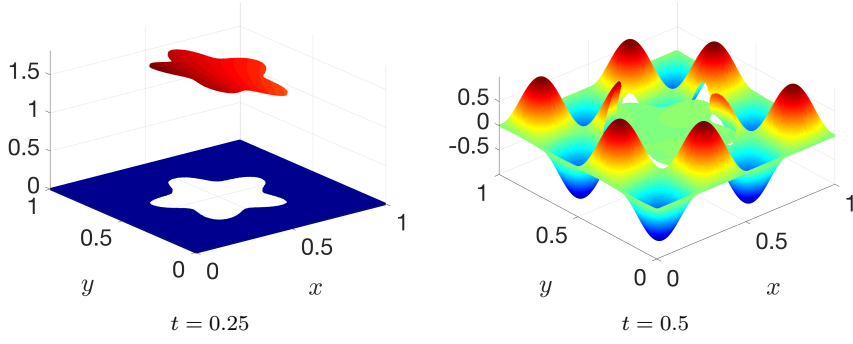


(a) second-order staggered FD scheme

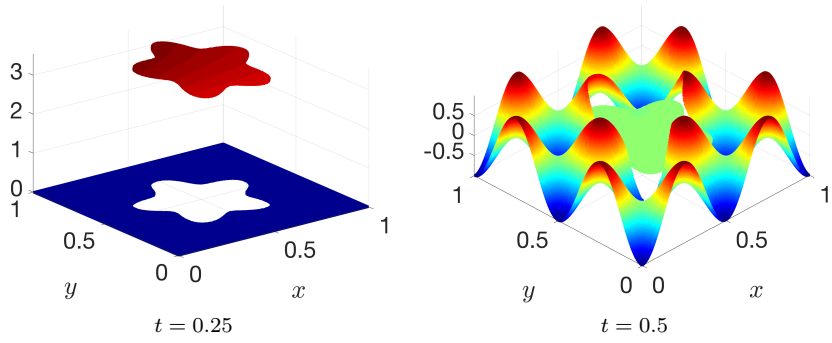


(b) fourth-order staggered FD scheme

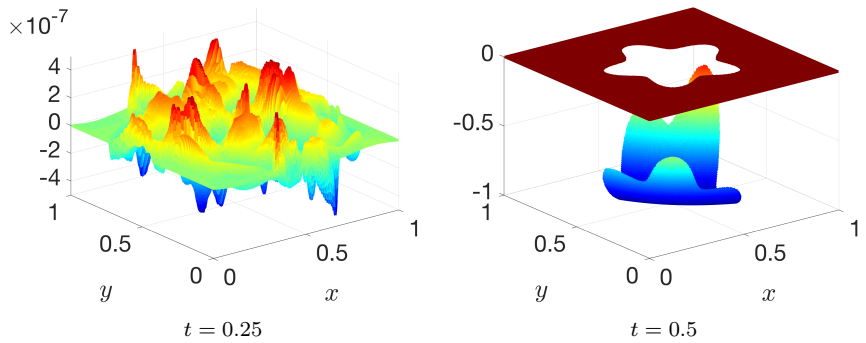
FIG. 6. Convergence plots for the problem with a manufactured solution and the star interface using a fourth-order approximation of the correction functions, and either a second-order or fourth-order staggered FD scheme. It is recalled that  $\mathbf{U} = [H_x, H_y, E_z]^T$ .



(a)  $H_x$

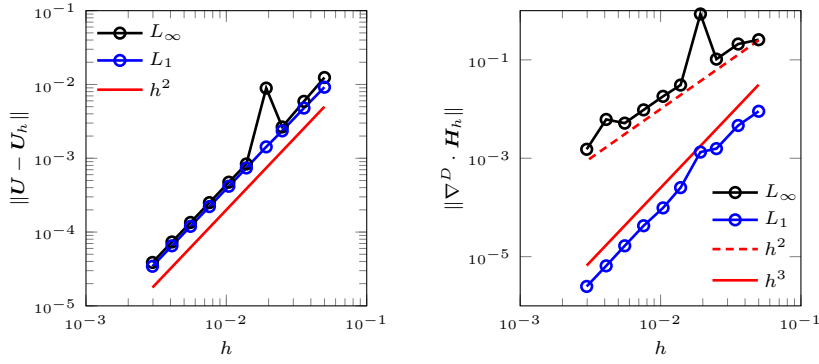


(b)  $H_y$

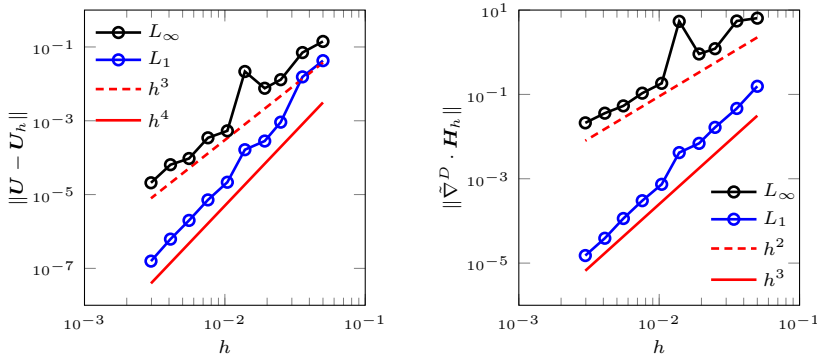


(c)  $E_z$

FIG. 7. The components  $H_x$ ,  $H_y$  and  $E_z$  at two time steps with  $h = \frac{1}{336}$  and  $\Delta t = \frac{h}{2}$  using a fourth-order staggered FD scheme with the CFM for the problem with a manufactured solution and the star interface.



(a) second-order staggered FD scheme



(b) fourth-order staggered FD scheme

FIG. 8. Convergence plots for the problem with a manufactured solution and the sharp interface using a fourth-order approximation of the correction functions, and either a second-order or fourth-order staggered FD scheme. It is recalled that  $U = [H_x, H_y, E_z]^T$ .

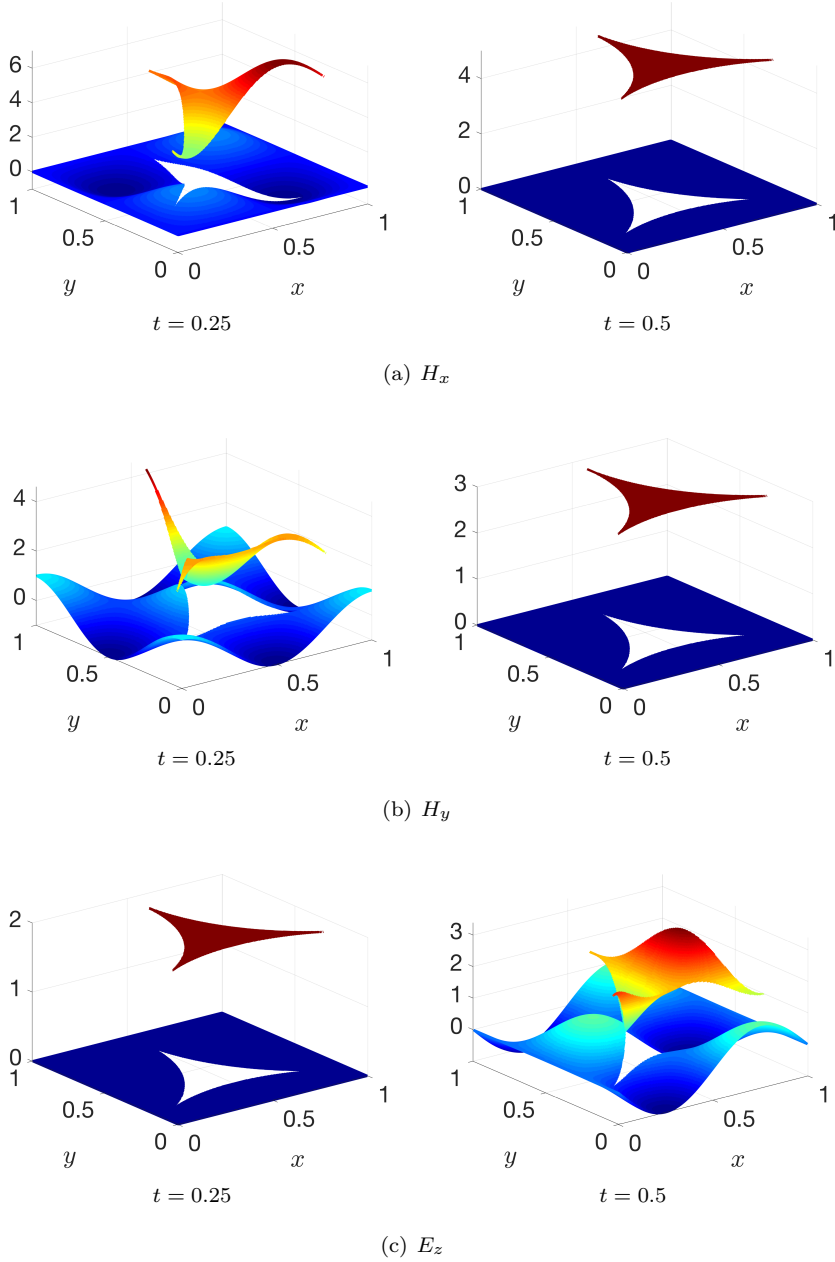


FIG. 9. The components  $H_x$ ,  $H_y$  and  $E_z$  at two time steps with  $h = \frac{1}{336}$  and  $\Delta t = \frac{h}{2}$  using a fourth-order staggered FD scheme with the CFM for the problem with a manufactured solution and the sharp interface.